Chern and Majorana modes of quasiperiodic systems

Indubala I. Satija[*] and Gerardo G. Naumis[†]

School of Physics Astronomy and Computational Sciences, George Mason University, Fairfax, Virginia 22030, USA and Departamento de Física-Química, Instituto de Física, Universidad Nacional Autónoma de México (UNAM), Apdo. Postal 20-364, 01000, México D.F., México

(Received 4 April 2013; revised manuscript received 22 July 2013; published 27 August 2013)

Different types of self-similar states are found in quasiperiodic systems characterized by topological invariants—the Chern numbers. We show that the topology introduces a competing length in the self-similar band edge states transforming peaks into doublets of size equal to the Chern number. This length intertwines with quasiperiodicity and introduces an intrinsic scale, producing Chern beats and nested regions where the fractal structure becomes smooth. Chern numbers also influence the zero-energy mode that, for quasiperiodic systems, which exhibit exponential localization, is related to the *ghost* of the Majorana: the remnant of the edge localized topological state that delocalizes at the onset to a topological transition. In superconducting wires, the exponentially decaying profile of the edge localized Majorana modes also encode fingerprints of the Chern states that reside in close proximity to zero energy.

DOI: 10.1103/PhysRevB.88.054204 PACS number(s): 71.23.Ft, 05.30.Rt, 74.78.−w, 73.43.Nq

I. INTRODUCTION

Quasicrystals (QC) are fascinating ordered structures exhibiting self-similar properties and long range order with regular Bragg diffraction[1] characterized by a hierarchical set of peaks. The revelation that these aperiodic crystals belong to topologically nontrivial phases[2] of matter is an exciting development that opens avenues in the frontiers of topological insulators.[3] Insulating in the bulk but conducting along the edges, topological insulators are exotic states of matter that support topologically protected gapless boundary modes and their number equals[4] the topological integer, the Chern number.[5] Key to the topological characterization of QCs is the translational invariance, that shifts the origin of quasiperiodic order,[2] which manifests as an additional degree of freedom relating QCs to higher dimensional periodic systems. Topological description of QCs requires an ensemble of such systems and can be characterized by the Chern number in view of their mapping to higher dimensions. An explicit demonstration of transport, mediated by the edge modes, has been demonstrated by pumping light across photonic QC.[2,6,7]

This paper studies an interplay between two exotic phenomena in quasiperiodic lattices: self-similar fractal patterns and nontrivial topology of band insulating states. In sharp contrast to prior studies[2,7] that developed the framework for topological characterization of QCs, the focus of this paper is the understanding of how topology and quasiperiodicity coexist. Here we elucidate a manifestation of the topology that is unique to QCs. In one-dimensional (1D) QCs, we show that the *band edge modes* encode topological invariants in their spatial profiles. Characterized by golden mean incommensurability, the central peak and the subpeaks of the band edge states split into doublets of size equal to the Chern number. This splitting which we refer to as *Chern dressing* is accompanied by new spatial patterns that include regions where the wave function varies smoothly. In other words, the topology generates nonfractal local regions of sizes dictated by the Chern numbers embedded in self-similar structure. This is reminiscent of the periodic orbits coexisting with chaotic dynamics. The Chern numbers also leave their fingerprints on the momentum distribution of particles, the observables that can be measured in experiments involving ultracold gases. These topological fingerprints in the band edge modes and the momentum distribution are found in the Harper and Fibonacci, as well as in generalized models that interpolate between these two.[7,8]

Quasiperiodic p-wave superconducting systems[9] provide another perspective on the Majorana, zero-energy topologically protected modes at the ends of infinitely long wires.[10] These modes have been the subject of very intense studies due to their potential applications in quantum computing. We show that in QCs where quasiperiodicity induces localization, fluctuations about exponentially localized zero energy modes describe Majorana at the onset to a topological phase transition. This extinction of the Majorana mode, which we refer to as *Majorana ghost*, as well as the exponentially decaying profile of the Majorana modes encode Chern-4 topology in view of their close proximity in energy. The shadowing or influence of one topological state to another is one of the intriguing aspects of quasiperiodic lattices that support both the Chern and the Majorana modes.

II. QUASIPERIODIC LATTICES AND CHERN NUMBERS

We consider a 1D chain of spinless fermionic atoms in a lattice described by the Hamiltonian,

$$H(\phi) = \sum_n t c_n^\dagger c_{n+1} + \text{H.c.} + \sum_n V_n(\phi) c_n^\dagger c_n. \qquad (1)$$

Here, $c_n^\dagger$ is the creation operator for a fermion at site n and t is the nearest-neighbor hopping amplitude. In our studies we have investigated a generalized potential that interpolates between the Harper and the Fibonacci model.[7] Here we will restrict ourselves to the Harper model with $V_n = 2\lambda \cos(2\pi(\sigma n + \phi))$, an incommensurate potential characterized by an irrational number σ which we take to be the inverse golden mean $[(\sqrt{5}-1)/2]$. Here λ controls the strength of quasiperiodic disorder and ϕ is an arbitrary phase. The eigenvalue equation, namely the Harper equation,

$$t\left(\psi^r_{n+1} + \psi^r_{n-1}\right) + 2\lambda \cos(2\pi(\sigma n + \phi))\psi^r_n = E\psi^r_n, \qquad (2)$$

exhibits a self-similar spectrum and wave functions[11,12] at $\lambda = t$. This self-dual point is the critical point for quasiperiodic disorder-induced quantum phase transition from extended to exponentially localized phase.[11]

This incommensurate system is studied by approximating σ by a sequence of rational approximates: the ratio of two consecutive Fibonacci numbers. The Fibonacci sequence is defined by $F_0 = 0$, $F_1 = F_2 = 1$, and $F_n = F_{n-1} + F_{n-2}$. For any rational approximant $\sigma = p/q = F_{n-1}/F_n$, the system consists of F_n bands and $F_n - 1$ gaps. The eigenstates of the incommensurate system are obtained as a limiting case of Bloch states of periodic system with period $q = F_n$ as $n \to \infty$, characterized by the Bloch vector k.

In parallel with the well known[5] formalism of quantized Hall conductivity for a 2D system, one can define an *adiabatic conductivity*, $\sigma_\Phi = \frac{e^2}{h} C_r$, for a 1D ensemble $H(\phi)$, of chains with a periodic boundary condition, where

$$\sigma_\Phi = \frac{e^2}{h} \mathrm{Im} \sum_{l=1}^{r} \int d\phi \left[\int dk \sum_{n=1}^{q} \partial_k \left(\psi_n^l\right)^* \partial_\phi \psi_n^l \right]. \qquad (3)$$

Here r labels the gap characterized by a Chern number, C_r, and integration over ϕ corresponds to an ensemble average of chains[7] related to each other by translation using phason shifts.[13,14] However, the quantity in the square bracket, the *Chern density*, in Eq. (3) is independent of ϕ, and therefore Chern number can be associated with any $H(\phi)$. This is in contrast with the rational σ, where the Chern density and the energy E depend upon ϕ and therefore the Chern number is associated only with the whole family of 1D systems, and that a single periodic system belongs to the trivial phase.

III. CHERN DRESSED SELF-SIMILAR WAVE FUNCTIONS

We now show that topology introduces a new length equal to the Chern number in the band edge states. Figure 1 shows numerically obtained self-similar wave functions for the band edge modes for topologically trivial and Chern-4 states, using a rational approximant of the inverse golden mean with a periodic boundary condition. These spatial profiles consist of a central or main peak and secondary peaks at distances given by Fibonacci numbers from the central peak. The wave functions display self-similarity as the structure around subpeaks approaches a scaled version of the structure around the central peak. A blowup of the region near any peak reveals new patterns. The most important feature associated with the primary as well as the secondary peaks is the Chern dressing as all peaks exhibit double-peak structures of sizes equal to the Chern number as illustrated further in Fig. 2.

To understand Chern dressing, we begin with Thouless[15] analysis of band edge states which identifies these wave functions as states of definite parity, with symmetry points about $n = 0$ or $n = q/2$. In other words, the rth band edge state shows the property $\psi_{n_1(r)} = \pm\psi_{n_2(r)}$ [$n_1(r) = -n_2(r)$ for center of symmetry about $n = 0$]. This symmetry where each site is paired with another site provides a starting point to understand the Chern dressing. We first consider the limit $\lambda \to \infty$, where due to exponential localization only the dominant peaks survive. In this case the wave function is given by $\psi_n^r(\pm) = \frac{1}{\sqrt{2}}(\delta_{n,n_1(r)} + e^{i\beta_\pm}\delta_{n,n_2(r)})$.[16,17]

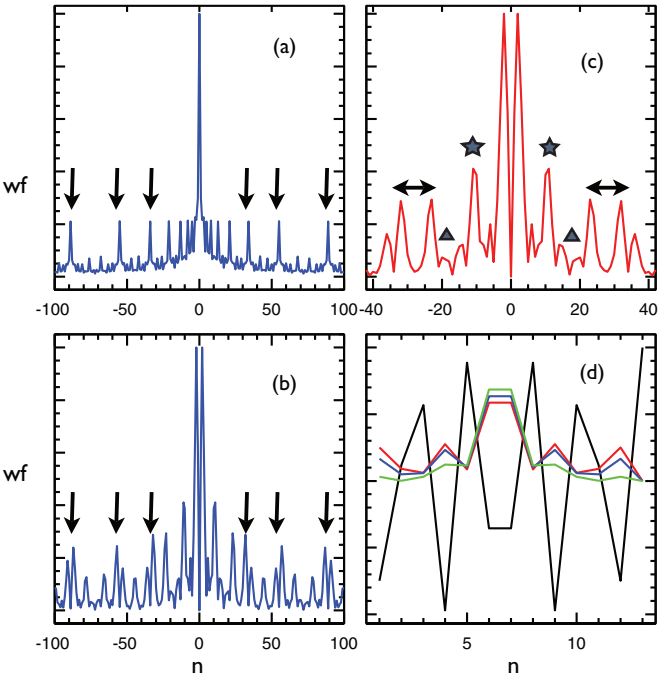

FIG. 1. (Color online) Magnitudes of the wave functions for the topologically trivial ground state (a), and the topologically nontrivial Chern-4–band edge state (b) at the critical point. The vertical arrows show the Fibonacci sites which are Chern dressed for the topological states. Note that the asymmetrically split Fibonacci peaks regain symmetry as one moves far from the center. Blowup of the region near the peak for Chern-4 state (c), showing structures consisting of dimerized peaks (star), distorted M-shaped regions (triangle), and regions separated by 9-sites (double arrow) where the wave function varies smoothly. Panel (d) shows on-site potential (black) and the Chern-1 wave function for $\lambda = 1, 1.1, 1.5$ (from bottom-top), illustrating our key observation that the location of the peaks is independent of λ.

It has been shown that the Chern number is given by $C_r = |n_1(r) - n_2(r)|$, corresponding to the spacing between the two localization centers. Here $\beta_+ = -(C_r - 1)\pi$ and $\beta_- = -C_r\pi$ are relative phases for the upper and lower band edges, respectively. We note that the cosine potential also has a pairing property, that is, for every site m_1 there exists a site m_2 such that $V(m_1) = V(m_2)$. Since for $\lambda \to \infty$ the eigenvalues are $E_r(\phi) = -2\lambda \cos(2\pi\sigma r + \phi) = V(n_1(r)) = V(n_2(r))$ and each eigenstate is simultaneously localized at $n = n_1(r)$ and $n = n_2(r)$; thus the spacing between the two localization centers is equal to the distance between the paired sites of the potential. Therefore, as we sort the eigenvalues or the potential, we can associate to each Chern number C_r a unique pair of sites $[n_1(r), n_2(r)]$ of the potential.

We will now argue that the Chern dressing illustrated above for $\lambda \to \infty$ also occurs for finite λ including $\lambda = t$ for the central as well as for subpeaks. This is in contrast to the rational σ case where Chern-dressed states, referred to as Chern-dimers,[17] exist only in the limit of large λ. Our key observation [illustrated in Fig. 1(d) for Chern-1 state] is that the locations of the (local) dominant peaks remain unchanged with λ. In other words, for all eigenstates, the wave function has maximum amplitude at sites given by the ordered pair of sites

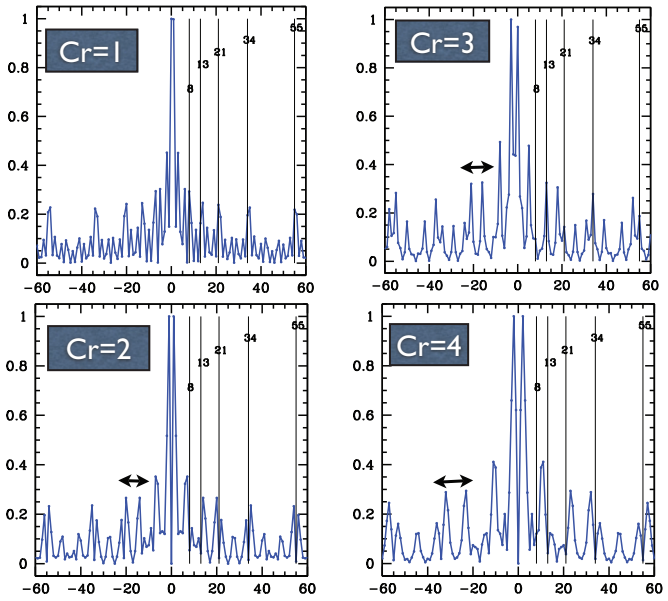

FIG. 2. (Color online) Spatial profile of Cherns 1–4 near the central peak. Vertical lines mark the Fibonacci locations which are Chern dressed, seen clearly once one moves away from the central peak. Lines with double arrows mark some of the regions where the magnitude of the wave functions vary smoothly.

that describe localization centers for $\lambda \to \infty$ all the way down to $\lambda = 1$ where the system exhibits power-law localization.

The key to the hierarchical manifestation of topology is the fact that the symmetry of the band edge wave functions about $n = 0$ or $n = q/2$, as discussed earlier, manifests asymptotically at all sites with an index that coincides with a Fibonacci number (Fibonacci sites), and the sites between the two consecutive Fibonacci spaced sites. This is a direct consequence of the number theory as $\lim_{m\to\infty} V(F_m) = V(0)$, since $V(F_m) = 2\lambda \cos(2\pi\sigma^{m-1})$ and $\sigma^m \to 0$ for $\sigma < 1$.

Briefly, the proof of the existence of Chern-dressed self-similar states as outlined above is based on a combination of Thouless's results about special symmetry of band edge states about $n = 0$ that demands localization at two sites simultaneously and the number theoretical argument that extends Thouless's analysis to every Fibonacci site. These arguments associate a unique integer, namely the distance between two localization centers with each band edge state. The argument that connects this integer to Chern number consists of two parts: rigorous proof that the distance between the localization center is the Chern number for $\lambda \to \infty$ and the empirical observation that this must also be valid for finite λ as the localization centers are independent of λ.

We recall that all previous studies of self-similar wave functions of QCs have been carried out for special points of the spectrum such as midband points[12] or the band edge points corresponding to maximum or minimum energy states. Such states are topologically trivial. These studies describe incommensurate states as consisting of a central or main peak and a sequence of subpeaks separated by Fibonacci distances from the central peak. For subpeaks far from the central peak, the ratio of subpeaks to central peak intensity approaches a well defined universal ratio. Topological states exhibit all these above mentioned features with additional structures such as Chern dressing and smooth regions embedded in the fractal pattern.

Figure 2 further illustrates Chern-dressed band edge states corresponding to Cherns 1–4, where peaks split into doublets of size equal the Chern number. The splitting is symmetrical for the central peak while the subpeaks away from the center split asymmetrically. However, the symmetry is restored as one moves farther from the main peak and, asymptotically, the Chern splitting occurs symmetrically. Another striking aspect associated with all self-similar band edge states is the existence of windows where the wave function varies smoothly with the lattice sites. These smooth regions are typically found to be associated with the reduction of Fibonacci spacings, $F_n \to F_n - C_r$, due to Chern splittings. The observed narrow windows where the fractal structure is wiped out include dimerized sites for Chern-1 band edge states where the wave functions at two consecutive sites have (asymptotically) equal intensity, a non-Fibonacci region of size $6(6 = 8 - 2)$ for the Chern-2 case and region of size $9(9 = 13 - 4)$ for the Chern-4 case. For Chern-3 case, the corresponding region has a size 5 $(5 = 8 - 3)$ as clearly marked in the figure. The smoothening is seen with higher clarity either at the center or as one moves away from the peaks. The appearance of such local regions of size controlled by the topological invariant is rather striking and signals a very unique role of topology, namely smoothening of the fractal structures. In our detailed study of band edge states with higher Chern states, the smooth regions were found to be confined to small regions. Analogous to periodic orbits underlying chaotic sea or crystalline symmetry patterns embedded in quasiperiodic lattices, smooth patterns nested[18] in fractal wave functions are fascinating and detailed understanding of what determines the sizes of these regular patterns remains elusive.

Figure 3 shows evidence of the self-similar pattern with scale invariance $x \to \sigma^3 x$, which corresponds to patterns repeating after every third Fibonacci spacing. Here we note that the pattern is symmetrical about the center and the central structure consists of one of the three new patterns discussed in the paper. The origin of this symmetry and the period-3 behavior is rooted in number theory. To illustrate this, we note that $F_n = F_{n-2} + F_{n-3} + F_{n-2}$. Therefore, the spatial patterns separated by F_n can be viewed as consisting of two regions: the central part of size F_{n-3} that sandwiches the two side patterns of length F_{n-2}, symmetrically placed about the center. The pattern repeats every third Fibonacci spacing as shown in the figures. The central part is identified with one of the three possible "structures" obtained by splitting of $F_n > C_r$.

IV. CHERN BEATS

Chern splitting of the peaks at Fibonacci sites introduces a beat frequency, which we will refer to as *Chern beats*, in the spatial patterns of the quasiperiodic lattices. We show that for the lower band edges, with $\lambda \leqslant 1$, $\psi_n^r \approx \cos(\pi C_r n/q)\Psi_n^0$, where Ψ_n^0 is the ground state wave function. We note that a similar expression can be found for upper band edges. This is the familiar standing wave at the band edges and for incommensurate lattices has its period controlled by the Chern numbers and demonstrates that the Chern number modulates the existing length scales of the quasiperiodic system.

We start by observing that the ground state wave function, ψ_n^0 for $\lambda \geqslant 1$, has most of its amplitude at Fibonacci sites in order to reduce the energy. Also, the state needs to be symmetric about zero in order to avoid having a node. Therefore, such a wave function can be written as

$$\psi_n^0 \approx \sum_p A_p[\delta(n - F_p) + \delta(n + F_p)]. \tag{4}$$

Using similar reasoning, the band edge states in view of Chern dressing can be described as

$$\psi_n^r \approx \sum_{p,n}\left[A_{p+C_r/2}\delta\left(n - F_p - \frac{C_r}{2}\right) + A_{p-C_r/2}\delta\left(n - F_p + \frac{C_r}{2}\right)\right] \pm \sum_{n,p}\left[A_{p+C_r/2}\delta\left(n + F_p - \frac{C_r}{2}\right) + A_{p-C_r/2}\delta\left(n + F_p + \frac{C_r}{2}\right)\right].$$

In view of asymptotic symmetry of the Chern splitting, we assume that $A_{p-C_r/2} \approx A_{p+C_r/2} \approx A_p$. Here $\pm$ respectively refers to the lower and the upper band edges.

The Fourier transform of ψ_n^r, denoted as $\Psi_m^r = \sum_m \psi_n e^{2\pi nm/q}$, is given by

$$\Psi_m^r(\pm) \approx \sum_p A_p[e^{i2\pi m(F_p + C_r/2)/q} + e^{i2\pi m(F_p - C_r/2)/q}] \pm \sum_p A_p[e^{-i2\pi m(F_p - C_r/2)/q} + e^{-i2\pi m(F_p + C_r/2)/q}],$$

where $\Psi(\pm)$ are given by

$$\Psi_m^r(+) \approx \cos(\pi m C_r/q)\sum_p 4A_p \cos(2\pi m F_p),$$

$$\Psi_m^r(-) \approx \cos(\pi m C_r/q)\sum_p 4iA_p \sin(2\pi m F_p).$$

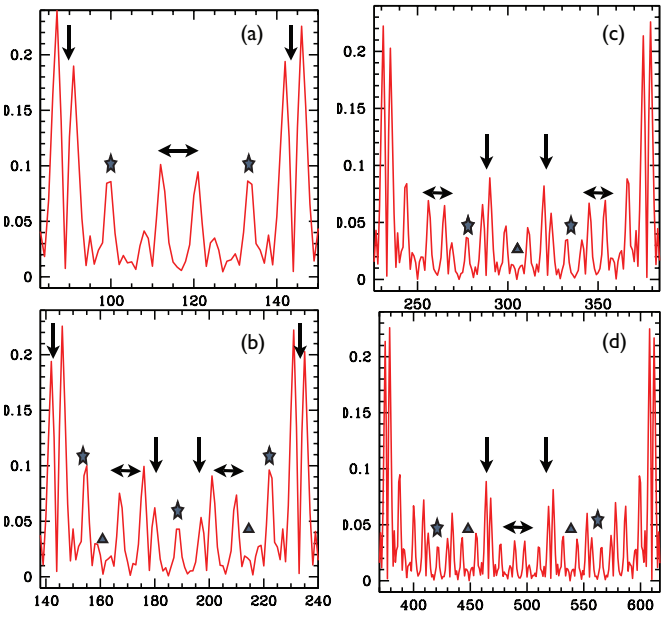

FIG. 3. (Color online) (a)–(d) respectively show spatial profile of the band edge modes for Cherns 4 separated by Fibonacci sites 89, 144, 233, and 377. The similarity between the patterns separated by 89 and 377, corresponding to three generations of Fibonacci separations, is clearly seen in the figure.

The topologically trivial states with $C_r = 0$ correspond to $r = 0$ and $r = q$ that respectively describe the minimum and the maximum energy states. Therefore, the upper and the lower band edge states can be written as a modulation of topologically trivial states $\Psi(E_{\min})$ and $\Psi(E_{\max})$:

$$\Psi_m^r(+) \approx \cos(\pi m C_r/q)\Psi_m(E_{\min}),$$
$$\Psi_m^r(-) \approx \cos(\pi m C_r/q)\Psi_m^q(E_{\max}).$$

Therefore, band edge density is given by

$$\rho(m) \approx \tfrac{1}{2}\rho^0(m)[1 + \cos 2\pi\kappa_r m], \tag{5}$$

where $\kappa_r^{-1} = \frac{q}{C_r}$ are the Chern beats, the topological length scales leading to spatial modulation of the quasiperiodic ground states with density ρ^0. In other words, topological states can be viewed as Chern-modulated ground states. Therefore, a length scale rooted in topology may underlie a whole class of physical phenomena, and the *mode beating* that has been observed in quasiperiodic systems[19] may be an example of this.

V. MOMENTUM DISTRIBUTION ENCODES TOPOLOGY

For a many body system of fermions, the topological fingerprints are also encoded in the momentum distribution: $n(k) = \sum_m^r |\eta_m^k|^2$, where η_m^k is the Fourier transform of the single particle wave function $\psi_l^m = \sum_k \eta_m^k \exp^{ikl}$ and the index r refers to the location of the Fermi level in the rth gaps. The flat momentum distribution, characteristic of the insulating state, develops wiggles, seen in Fig. 4, that are somewhat correlated with the topological invariant. This relationship becomes very transparent in the limit $\lambda \to \infty$ as the momentum distribution exhibits sinusoidal oscillations, $n(k) = \nu_r[1 + \frac{1}{q}\cos(2akC_r)]$,[17] where ν_r is the filling factor, namely the density of particles, that fills up all states below the the rth gap characterized by the Chern number C_r. These wiggles in the momentum distributions are a manifestation of Friedel oscillations[20,21] induced by quasiperiodic disorder. We note that, in view of self-duality, the momentum distribution also describes the density profile with $k = \langle \sigma n \rangle$, where $\langle x \rangle$ denotes the fractional part of x. Furthermore, the fermionic density also describes the density for a gas of hard core bosons which have been realized in cold atomic gases.[22]

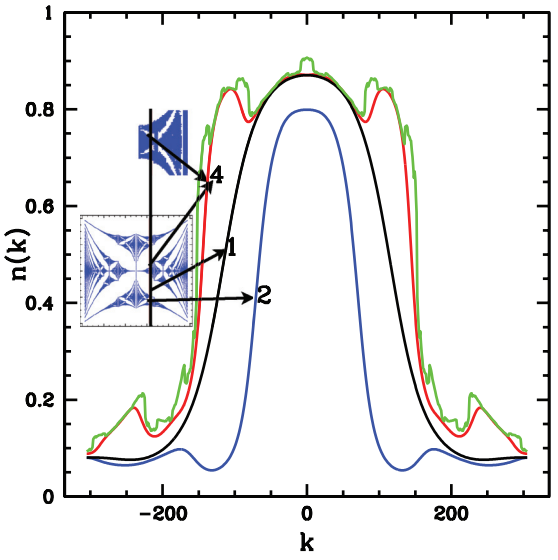

FIG. 4. (Color online) Fingerprints of Chern numbers in the momentum distributions with Fermi levels in the gaps characterized by $C_r = 1,2,4$. The outermost curve (green) shows a nontopological many body state corresponding to filling factor of half, that resembles the Chern-4 band insulating state in view of close proximity in energy. Gaps characterized by these Chern numbers are shown in the slice of the butterfly spectrum[31] at the irrational flux (indicated by vertical line). Small inset above the butterfly is the blowup of the butterfly slice that contains Chern-4 gap, showing its proximity to the zero-energy state that exists at the center of the spectrum.

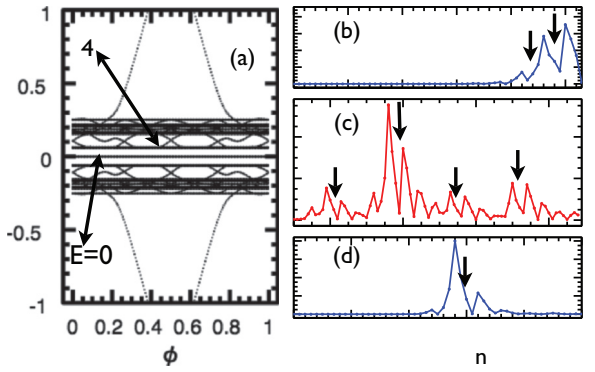

FIG. 5. (Color online) For $\Delta = 0.2$, (a) shows energy spectrum at $\lambda = 1$ where lines with arrows mark $E = 0$ and Chern-4 band edge states, illustrating their proximity in energy. The 4-chiral modes in the gap are distinctly visible. Panels (b)–(d) respectively show the magnitude of wave functions for $E = 0$ state below ($\lambda = 1$), at ($\lambda = 1.2$), and above ($\lambda = 1.5$) the transition. The spatial profile of Majorana shows (b) decaying set of peaks separated by 4. The delocalized critical (c) and topologically trivial mode above criticality (d) shows Chern-4 dressing, all highlighted by lines with arrow.

VI. CHERN AND MAJORANA MODES

We will now discuss quasiperiodic systems that support Majorana modes[10] in addition to Chern-dressed band edge states. The system under consideration is a variant of the Harper Hamiltonian, describing a p-wave superconducting wire, in the presence of quasiperiodic spatial inhomogeneity:[9]

$$H_s = \sum_n [-\omega c_n^\dagger c_{n+1} + \Delta c_n^\dagger c_{n+1}^\dagger + \text{H.c.} + V_n(\phi) c_n^\dagger c_n]. \quad (6)$$

Here ω is the nearest-neighbor hopping amplitude and Δ is the p-wave pairing amplitude, both taken to be real constants. The eigenvalue equation of the system is a coupled set of equations for two-component wave functions (f_n, g_n),[23]

$$(\omega - \Delta) f_{n+1} + (\omega + \Delta) f_{n-1} + V_n(\phi) f_n = E g_n, \quad (7)$$

$$(\omega + \Delta) g_{n+1} + (\omega - \Delta) g_{n-1} + V_n(\phi) g_n = E f_n. \quad (8)$$

The quasiperiodic system (6) has been shown to exhibit localization transition[9,24] similar to that of the Harper model at $\lambda_c = \omega + \Delta$, where the critical point accompanied by the appearance of the $E = 0$ mode also describes the onset to a topological phase transition.

We first show that the zero-energy state in the superconducting system at criticality is related to the zero-energy exponentially localized states of the Harper equation.[25] From Eq. (2), it follows that the fluctuations η_n about the exponentially decaying envelope, $\psi_n = e^{-n\xi}\eta_n$, satisfy the following equation, with $\xi = \ln(\lambda/t)$ being the inverse localization length:

$$t(e^{-\xi}\eta_{n+1} + e^{\xi}\eta_{n-1}) + 2\lambda \cos(2\pi(\sigma n + \phi))\eta_n = E\eta_n. \quad (9)$$

At $\lambda = \lambda_c$, Eqs. (7), (8), and (9) become equivalent for the $E = 0$ state.[25] Therefore, fluctuations η_n in the localized envelope of the $E = 0$ state of Harper are related to the delocalized states that correspond to the extinction of Majorana, the Majorana ghost, at the threshold of the topological phase transition.

In a finite chain, for $\lambda < \lambda_c$, the quasiperiodic model (6) hosts Majorana mode at $E = 0$. As seen in Fig. 5, the $E = 0$ mode exists in close proximity to the Chern-4 mode and its spatial profile is strongly influenced by the band edge state. First, the envelope of the edge localized Majorana has a decaying set of peaks separated by four lattice spacing. Furthermore, at criticality the zero mode delocalizes, and its spatial profile is Chern dressed as all peaks are doublets of size 4. In the nontopological localized phase, the interior localized mode also exhibits double peak. The fact that the Majorana as well as its remnants encode the Chern-4 topological invariant is intriguing and perhaps a rare example of interplay of two distinct topological effects.

We note that the Chern-4 shadowing has a very simple origin, namely, the Chern-4 band edge state is the smallest Chern number state that resides in close proximity to the zero mode. This is valid only for the incommensurate parameter and equals the inverse golden mean that is used here. For other irrationals, there will be a similar effect provided a prominent (small Chern state) exists in proximity to the zero-energy mode and it need not be the Chern-4 state.

VII. SUMMARY

The interplay between topology and quasiperiodicity provides a remarkable example of competing periodicities where Chern numbers, the aliens in Fibonacci landscape, adapt to the quasiperiodic environment. Our results are valid for

all irrationals with a periodic tail in the continued fraction expansion.[12] The renormalization scheme that incorporates the Chern length, preserving scale invariance, remains an open problem. In addition to photonic systems, QCs described by the Harper equation have been realized in ultracold atomic gases.[26] From the cold-atom point of view, these lattices have been investigated in various contexts.[21,27] Photonic experiments which can simulate tight binding lattice Hamiltonians using coupled rings resonators may provide an ideal setup to observe Chern splitting.[28] In these experiments, the on-site potential can be controlled by changing the size of the rings and a direct measurement of the wave function can be performed.

Superconducting quantum wires have been shown to be promising candidates for realizing Majorana fermions.[29] The Chern shadowing of the Majorana mode is a rather unique observation that is intriguing and its importance in the context of the current hunt for the Majorana is not obvious. However, characteristics described here may pave the way to some new types of investigations in studies of Majorana modes and may stimulate a different line of research in the hunt for new exotic states of matter that involve an interplay between the Majorana and the Chern modes. Finally, exploring the role and manifestation of topology in interactioning QP systems, particularly in the context of many-body localization that have been recently studied,[30] may be important.

Fractal patterns in quantum systems are rare and arouse a great deal of excitement as evident from the Hofstadter butterfly spectrum,[31] whose experimental confirmation was reported recently.[32] This extraordinary quantum effect where complicated structure of gaps, each characterized by a unique Chern number, are arranged in a fractal pattern, creates a new frontier to explore unknown electrical properties. Our key findings, such as Chern dressed self-similar patterns, Chern beats, Chern-4-shadowed Majorana, and topology that smoothen fractals are some of the intriguing results that may prove vital in exploration of topological states that exist in quasiperiodic systems.

ACKNOWLEDGMENTS

We would like to thank M. Hafezi for discussion regarding experimental realization of Chern-dressed states in photonic experiments. This research is supported by ONR and DGAPA IN102513.

*isatija@gmail.com
†naumis@fisica.unam.mx

[1] C. Janot, *Quasicrystals*, 2nd ed. (Clarendon, Oxford, 1994).
[2] Y. E. Kraus, Y. Lahini, Z. Ringel, M. Verbin, and O. Zilberberg, Phys. Rev. Lett. **109**, 106402 (2012).
[3] M. Z. Hasan and C. L. Kane, Rev. Mod. Phys. **82**, 3045 (2010).
[4] Y. Hatsugai, Phys. Rev. Lett. **71**, 3697 (1993).
[5] D. J. Thouless, M. Kohmoto, M. P. Nightingale, and M. den Nijs, Phys. Rev. Lett. **49**, 405 (1982).
[6] M. Verbin, O. Zilberberg, Y. E. Kraus, Y. Lahini, and Y. Silberberg, Phys. Rev. Lett. **110**, 076403 (2013).
[7] Y. E. Kraus and O. Zilberberg, Phys. Rev. Lett. **109**, 116404 (2012).
[8] G. G. Naumis and F. J. Lopez-Rodriguez, Physica B **403**, 1755 (2008).
[9] W. DeGottardi *et al.*, Phys. Rev. Lett. **110**, 146404 (2013); X. Cai *et al.*, arXiv:1208.2532.
[10] A. Kitaev, Ann. Phys. (NY) **321**, 2 (2006).
[11] S. Aubry and G. Andre, Ann. Isr. Phys. Soc. **3**, 133 (1980).
[12] S. Ostlund and R. Pandit, Phys. Rev. B **29**, 1394 (1984).
[13] G. G. Naumis, C. Wang, M. F. Thorpe, and R. A. Barrio, Phys. Rev. B **59**, 14302 (1999); G. G. Naumis, *ibid.* **71**, 144204 (2005).
[14] D. Levine and P. J. Steinhardt, Phys. Rev. B **34**, 596 (1986).
[15] D. J. Thouless, Phys. Rev. B **28**, 4272 (1983).
[16] E. Fradkin, *Field Theories of Condensed Matter Systems* (Addison-Wesley, Redewood City, California, 1991), p. 287.
[17] E. Zhao, N. Bray-Ali, C. J. Williams, I. B. Spielman, and I. I. Satija, Phys. Rev. A **84**, 063629 (2011).
[18] G. Naumis and J. L. Aragon, Z. Kristallogr. **218**, 1 (2003).
[19] L. Dal Negro, C. J. Oton, Z. Gaburro, L. Pavesi, P. Johnson, A. Lagendijk, R. Righini, M. Colocci, and D. S. Wiersma, Phys. Rev. Lett. **90**, 055501 (2003).
[20] J. Friedel, Nuovo Cimento, Suppl. **7**, 287 (1958).
[21] A. M. Rey, I. I. Satija, and C. W. Clark, Phys. Rev. A **73**, 063610 (2006).
[22] B. Paredes, A. Wideara, V. Murg, O. Mandel, S. Folling, I. Cirac, G. V. Shlyapnikov, T. W. Hansch, and I. Bloch, Nature (London) **429**, 277 (2004).
[23] E. Lieb, T. Schultz, and D. Mattis, Ann. Phys. (NY) **16**, 407 (1961).
[24] I. I. Satija and M. M. Doria, Phys. Rev. B **39**, 9757 (1989); J. Ketoja and I. Satija, Physica A **219**, 212 (1995).
[25] J. A. Ketoja and I. I. Satija, Phys. Rev. Lett. **75**, 2762 (1995).
[26] V. Guarrera, N. Fabbri, L. Fallani, C. Fort, K. M. R. van der Stam, and M. Inguscio, Phys. Rev. Lett. **100**, 250403 (2008).
[27] R. Roth and K. Burnett, Phys. Rev. A **68**, 023604 (2003); R. Citro, A. Minguzzi, and E. Orignac, *ibid.* **78**, 013625 (2008).
[28] M. Hafezi, E. A. Demler, M. D. Lukin, and J. M. Taylor, Nature Phys. **7**, 907 (2011).
[29] V. Mourik, K. Zuo, S. Frolov, S. Plissard, E. Bakkers, and L. P. Kouwenhoven, Science **336**, 1003 (2012); X. Liu and J. K. Furdyna, Nature Phys. **8**, 795 (2012); C. W. J. Beenakker, Annu. Rev. Condens. Matter Phys. **4**, 113 (2013).
[30] S. Iyer, V. Oganesyan, G. Refael, and D. A. Huse, Phys. Rev. B **87**, 134202 (2013).
[31] D. Hofstadter, Phys. Rev. B **14**, 2239 (1976).
[32] C. R. Dean *et al.*, Nature **497**, 598 (2013).